Organic functionalisation and characterisation of single-walled carbon nanotubes

Prabhpreet Singh,[a] Stéphane Campidelli,[bc] Silvia Giordani,[bd] Davide Bonifazi,[be] Alberto Bianco[a] and Maurizio Prato*[b]

Received 9th January 2009
First published as an Advance Article on the web 22nd June 2009
DOI: 10.1039/b518111a

Since carbon nanotubes (CNTs) display unique structures and remarkable physical properties, a variety of applications have emerged in both materials and life sciences. In terms of applications, the functionalisation of nanotubes is extremely important, as it increases their solubility and processability, and combines the unique properties of single-walled carbon nanotubes (SWCNTs) with those of other classes of materials. A number of methods have been developed, which can be divided into two major approaches: (1) non-covalent supramolecular modifications, and (2) covalent functionalisation. In this *tutorial review*, we survey the covalent modification of SWCNTs with organic moieties, and illustrate the major analytical techniques routinely used to characterise the functionalised materials.

1. Introduction

Carbon nanotubes (CNTs) are cylinder-shaped macromolecules with a radius as small as a few nanometres. Historically, multi-walled nanotubes (MWCNTs) were the first to be characterised at an atomic resolution in 1991,[1] followed by their single-walled counterparts in 1993.[2] SWCNTs possess the simplest geometry (rolling of one single graphene sheet) and their diameters typically range from 0.7–2 nm. MWCNTs are instead composed of a concentric arrangement of many cylinders reaching diameters of up to 100 nm.

SWCNTs are usually produced by arc discharge of graphite, laser ablation, or gas-phase catalytic growth from carbon monoxide or other carbon sources.[3,4] The raw material usually contains nanotubes mixed with amorphous carbon and catalytic metal particles as impurities.

SWCNTs possess extraordinary mechanical properties such as a high Young modulus (estimated to be 1–5 TPa), high tensile strength (50–200 GPa), high elasticity and resilience, thermal conductivity and large aspect ratio (length to diameter).[3,4]

[a] *CNRS, Institut de Biologie Moléculaire et Cellulaire, Laboratoire d'Immunologie et Chimie Thérapeutiques, 15 Rue René Descartes, 67000, Strasbourg, France*
[b] *Dipartimento di Scienze Farmaceutiche and INSTM UdR Trieste, Università degli Studi di Trieste, I-34127, Trieste, Italy. E-mail: prato@units.it*
[c] *CEA, Laboratoire d'Electronique Moléculaire, IRAMIS/SPEC, 91191, Gif sur Yvette cedex, France*
[d] *School of Chemistry/Centre for Research on Adaptive Nanostructures and Nanodevices (CRANN), Trinity College Dublin, College Green, Dublin 2, Ireland*
[e] *Département de Chimie, Facultés Universitaires Notre Dame de la Paix, B-5000, Namur, Belgium*

Prabhpreet Singh

Prabhpreet Singh was born in Amritsar, India in 1978. He obtained his PhD in 2006 from Guru Nanak Dev University, Amritsar (India) under the supervision of Prof. Subodh Kumar working on the construction of molecular switches and logic gates based on organic molecules. He worked as a postdoctoral fellow in the group of Prof. Sandeep Verma at the Indian Institute of Technology, Kanpur, India (2006–2007). In 2007, he joined the group of Dr Alberto Bianco and is presently working as a postdoctoral fellow. His research interests include supramolecular chemistry, the synthesis and morphological studies of peptide scaffolds, and the functionalisation of carbon nanotubes.

Stéphane Campidelli

Stéphane Campidelli was born in 1974 in France. He obtained his "DEA" (MSc degree) in organic chemistry from the University of Aix-Marseille III (France) in 1998. After a short period in industry, he began his PhD in 2000 under the supervision of Prof. Robert Deschenaux at the University of Neuchâtel in Switzerland. His PhD dissertation was awarded by the "prix Syngenta Monthey". In 2004, he joined the group of Prof. Maurizio Prato at the University of Trieste (Italy) for a postdoctoral fellowship. In January 2007 he moved to CEA Saclay where he is currently working as a researcher.

SWCNTs can be either metallic or semiconducting depending on their chiral vectors. The possible defects that can be visualised in carbon nanotubes are: topological (*e.g.* the presence of pentagons or heptagons at the curvature sites and in the C framework), rehybridisation ($sp^2 \rightarrow sp^3$), incomplete bonding defects (vacancies and dislocations) and doping with elements other than carbon.[3,4]

SWCNTs have found a wide range of applications, from molecular electronics to field effect transistors, in microelectronics, optoelectronics, gas storage, sensing, field emission devices and components in high performance composites, nanobiotechnology, and nanomedicine.[4,5]

SWCNTs mostly exist in bundles due to the presence of strong intermolecular cohesive forces (0.5 eV nm^{-1})[3,4] between tube-to-tube contacts. This feature results in poor solubility in all solvents, which is an obstacle for the full exploitation of the SWCNT properties. For many applications, several protocols have been described in the literature to exfoliate and functionalise SWCNTs while generating individuals and/or small bundles.

In this tutorial review, we will focus our attention on recent developments and selected examples of organic transformations of SWCNTs, followed by a detailed description of the analytical techniques necessary to characterise the functionalised SWCNTs.

2. Organic functionalisation of SWCNTs

Although some of the applications discussed above can be realised through *in situ* growth or by the use of pristine SWCNTs, many other uses require solution phase processing and manipulations to achieve homogeneous dispersions within host materials. Often, an effective purification of the nanotubes is required before their further processing.

Two approaches have been developed for the covalent functionalisation of carbon nanotubes: (i) amidation and

Silvia Giordani

Silvia Giordani was born in Bergamo (Italy) in 1973. She obtained a "Laurea" from the University of Milano and a PhD in Chemistry from the University of Miami (USA). She then moved to Trinity College, Dublin (Ireland) with a Marie Curie post-doctoral Fellowship, and later to the University of Trieste with a Marie Curie re-integration grant. She has been awarded the SFI's "President of Ireland Young Researcher Award" and in September 2007 she joined the School of Chemistry at TCD as research lecturer. Her research interests focus on the synthesis of molecular switches and polymers, and the functionalisation of carbon nanotubes.

Davide Bonifazi

Davide Bonifazi was born in Guastalla (Italy) in 1975. After obtaining a Laurea from the University of Parma (1999), he joined the group of Prof. François Diederich at ETH Zürich (2000–2004). After a postdoctoral fellowship with Prof. Maurizio Prato at the University of Trieste (2004–2005), he joined the Department of Pharmaceutical Science as a visiting scientist. In September 2006, he joined the Department of Chemistry at the University of Namur as a junior professor of organic chemistry. His research interests focus on the synthesis of π-conjugated molecular scaffolds, molecular self-assembly, and the functionalization of porphyrins and carbon nanostructures.

Alberto Bianco

Alberto Bianco received his Laurea degree in Chemistry in 1992 and his PhD in 1995 from the University of Padova (Italy). As a visiting scientist, he worked at the University of Lausanne during 1992, at the University of Tübingen in 1996–1997, as an Alexander von Humboldt fellow, and at the University of Padova in 1997–1998. He currently is a research director at the CNRS in Strasbourg (France). His research interests focus on the development of carbon-based nanomaterials (carbon nanotubes and fullerenes) and their use. He is also on the advisory board of the Journal of Peptide Science.

Maurizio Prato

Maurizio Prato graduated in 1978 from the University of Padova, Italy, where he was appointed assistant professor in 1983. He moved to Trieste as an associate professor in 1992 and was promoted to full professor in 2000. He spent a year in 1986–1987 at Yale University, was visiting scientist at the University of California, Santa Barbara, in 1991–1992, and Professeur Invité at the Ecole Normale Supérieure in Paris, France, in July 2002. His research interests focus on the functionalisation chemistry of fullerenes and carbon nanotubes for applications in materials science and medicinal chemistry, and on the synthesis of biologically active substances.

esterification of oxidised SWCNTs; and (ii) addition chemistry to SWCNTs.

(i) The treatment of the crude material under strong acidic and oxidative conditions, such as sonication in a mixture of concentrated nitric and sulfuric acid, or heating in a mixture of sulfuric acid and hydrogen peroxide, results in the formation of short opened tubes with oxygenated functions (carbonyl, carboxyl, hydroxyl, *etc.*).[6] This approach represents a popular pathway for further modification of the nanotubes, since the acid functions can react with alcohols or amines to give ester or amide derivatives. (ii) The functionalisation of SWCNTs is not limited to the chemistry of carboxylic acid. More elaborate methods have been developed to attach organic moieties directly onto the nanotube sidewalls. These include cycloadditions, electrophilic and nucleophilic or radical additions, *etc.* A few reviews dealing with the chemistry of SWCNTs have recently appeared in the literature describing exhaustive or representative examples of covalent functionalisation.[7]

2.1 Amidation and esterification of oxidised SWCNTs

Amidation or esterification reactions can be carried out on oxidised SWCNTs by standard methods, either using acid chlorides as intermediates or carbodiimide-activated coupling. Haddon and his collaborators first reported a number of strategies leading to soluble SWCNTs through amidation reactions between shortened nanotubes and octadecylamine (**1**) and 4-tetradecylaniline (Scheme 1).[8a] The coupling was carried out *via* an acyl chloride intermediate obtained by the reaction of oxidised SWCNTs with oxalyl chloride or by the formation of zwitterions through an acid–base reaction. The octadecylamine groups present on the nanotubes act as solubilising agents and the conjugates are soluble in most organic solvents. To increase the water solubility of SWCNTs, the same group described covalent functionalisation with poly(*m*-aminobenzene sulfonic acid) (PABS) (**2**) *via* an amide link.[8b] The conductivity of the SWCNT–PABS co-polymer was much higher than that of the parent PABS. Following the method developed by Haddon, Pompeo and Resasco reported the coupling of glucosamine to the acyl chloride-activated nanotubes (**3**).[9] The solubility in water of the conjugates ranged from 0.1–0.3 mg mL^{-1}, depending on temperature.

This approach has been used by several groups for combining the SWCNT properties with those of other interesting materials. For instance, coupling SWCNTs with C_{60} fullerene generates unique structures, which have been studied for charge-transfer properties. Delgado *et al.*[10a] reported the first conjugated nanohybrid material (**4**) based on SWCNT–fullerene, by an amidation reaction between a carboxylic–SWCNT and an aniline–fullerene derivative. Along the same line, a grapevine nanostructure (**5**) was synthesised, based on SWCNT covalently functionalised with C_{60}, by an amidation reaction between the amino group on the fullerene and the oxidised SWCNTs.[10b] ESR spectroscopy revealed that the ground state electron-transfer occurred from SWCNTs to the C_{60} moieties. The cyclic voltammetric responses of the film remarkably resemble those of C_{60} derivatives in solution and exhibit reversible multiple-step electrochemical reactions. We reported the synthesis of several hybrid fullerene derivatives–SWCNT materials that combined [60]fullerenes with appended photoactive ferrocene or porphyrin functionalities and SWCNTs (**6**).[11] Detailed XPS investigations have documented the presence of [60]fullerene derivatives around the exo-surface of the oxidised SWCNT walls, exhibiting a characteristic photoelectron N 1s emission peak at 400.3 eV, typical of amide groups.

Many novel biosensor systems have been prepared based on functional SWCNTs.[12] SWCNTs were modified using 1,2-bis(10,12-tricosadiynoyl)-sn-glycero-3-phosphoethanolamine (DCPE) phospholipid (**7**), obtaining stable dispersions with uniform thickness.[13a] Baker *et al.*[13b] described covalently linked adducts of SWCNTs and DNA (**8**). The high stability and accessibility in hybridisation experiments indicates that DNA chains are chemically bound to the exterior surface of SWCNTs and are not wrapped around or intercalated within the nanotubes. These DNA–SWCNT adducts hybridise selectively with complementary sequences, with only minimal interactions with mismatched sequences. Sun and co-workers reported the functionalisation of SWCNTs with 2′-aminoethyl-β-D-galactopyranoside (**9**).[14a] These Gal–SWCNTs were highly efficient in capturing *E. coli* by interaction with receptors present on the cell surface of the pathogens. Papadimitrakopoulos and coworkers reported the covalent functionalisation of SWCNTs with flavin mononucleotide (FMN) (**10**).[14b] The emission of the FMN was quenched because of the strong π–π interactions between the aromatic flavin moiety and the SWCNT external surface, which caused a rearrangement of the dye configuration onto the SWCNT sidewalls. In recent years, more complex structures have been designed (*i.e.* organisation of nanotubes on electrode surfaces and attachment of electroactive/photoactive groups, semiconductor nanoparticles or attachment of modified flavin adenine dinucleotide co-enzyme) with the aim of finding applications either as biosensors or generators of photocurrents.[15]

The alternative functionalisation of SWCNTs by esterification of the carboxylic functions has been also extensively exploited. The covalent attachment of porphyrin units to SWCNTs (**11** and **12**) *via* an esterification reaction, yielding compounds soluble in polar organic solvents, was reported by different groups (Scheme 1). Baskaran *et al.*[16b] reported that in supramolecular donor–acceptor complex **12**, SWCNTs serve as an efficient electron acceptor component, as evidenced by substantial quenching of the porphyrin luminescence. Li *et al.*[16a] also reported that quenching of the fluorescence of the porphyrin units was strongly dependent on the length of the spacer between the nanotube and the chromophore. While no fluorescence quenching was observed for **11b**, in the case of **11a**, the fluorescence of the porphyrin was approximately 70% of that of the reference compound. This result could be attributed to the length and flexibility of the alkyl chain, which allows a better interaction between the nanotube and the porphyrin for **11a**.

Recently, Cosnier and Holzinger[17] also reported the esterification reaction of long alkyl pyrrole moieties to oxidised SWCNTs. The pyrrole–ester–SWCNTs **13** were dissolved in THF and electropolymerised by controlled potential electrolysis at 0.95 V.

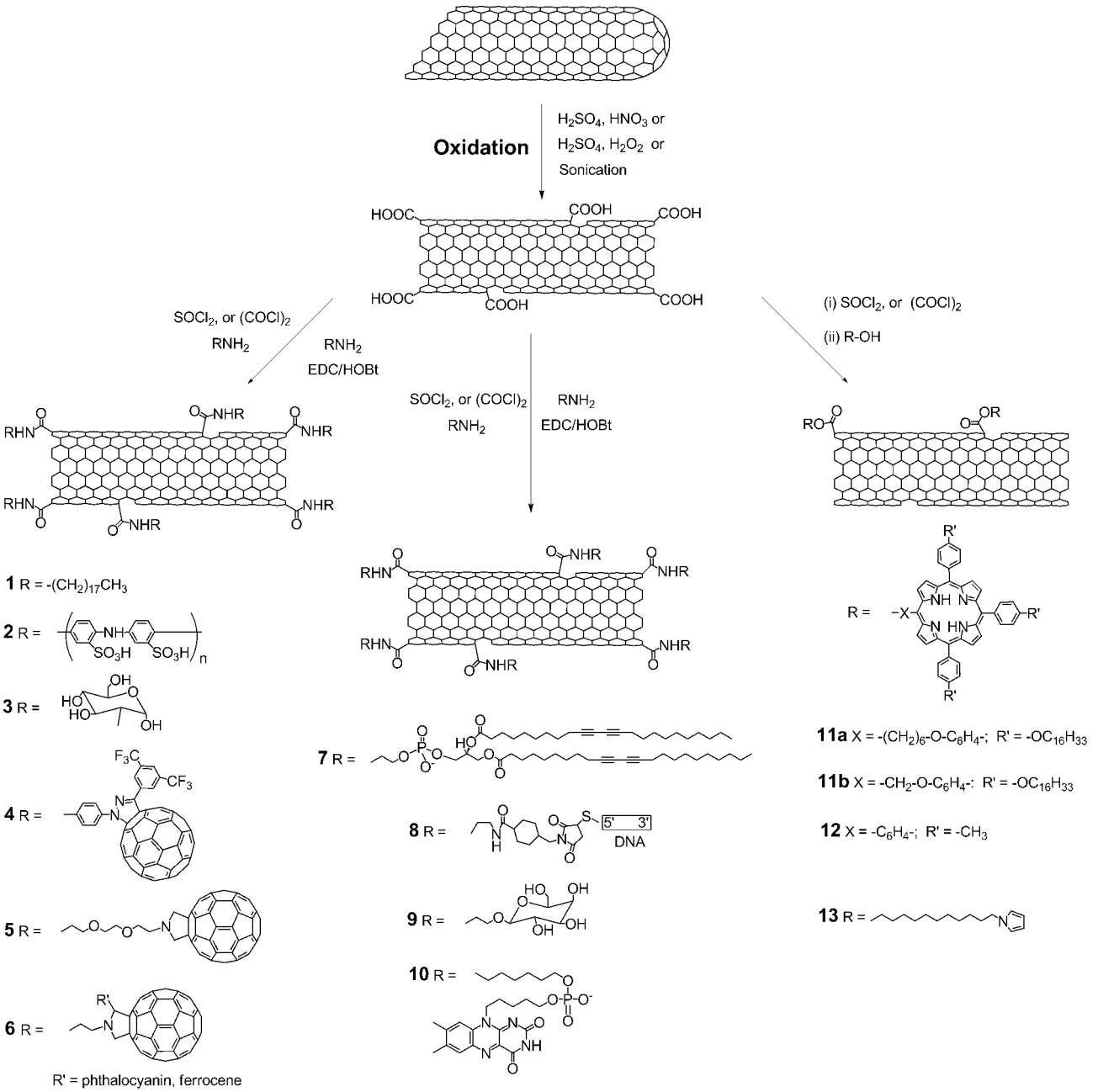

Scheme 1 Covalent functionalisation of SWCNTs following amidation and esterification reactions of carboxylic acid groups.

2.2 Addition chemistry to SWCNTs

In contrast to the esterification or amidation reactions of the acid groups of oxidised SWCNTs, the functionalisation of their sidewalls requires the use of highly reactive species. Ideal pristine SWCNTs possess two distinct regions, caps or tips and sidewalls, with different reactivity towards covalent chemical modifications. The presence of five-membered rings at the end of the nanotubes leads to a relatively higher reactivity, similar to fullerene. Functionalisation of the sidewalls is more difficult to accomplish. Addition reactions to carbon–carbon double bonds cause the transformation of sp^2- into sp^3-hybridised carbon atoms, which is associated with a change from a trigonal-planar local geometry to a tetrahedral geometry. This process is energetically more favourable at the tips due to their pronounced curvature, in marked contrast to the sidewalls with their comparatively lower curvature. In reality, nanotubes are not ideal structures, but rather contain defects formed during their synthesis; it is probable that reactions preferably occur near defect sites.[18a] Sidewall functionalisation has been achieved either on pristine or oxidised and/or modified SWCNTs.

2.2.1 Fluorination. Fluorination of SWCNTs with elemental fluorine at several different temperatures was first reported by Margrave and co-workers.[3a,18b] The bulk of the SWCNTs survive the fluorination process at temperatures between 150–400 °C, since at higher temperatures the graphitic

network appreciably decomposes. Fluorinated nanotubes (abbreviated as F-SWCNTs) contain one fluorine atom for every two carbon atoms. Once fluorinated, F-SWCNTs can be defluorinated with anhydrous hydrazine. The fluorination of the nanotubes drastically enhances the reactivity of the sidewalls and subsequent modifications are possible. It was demonstrated that the sidewall alkylation of F-SWCNTs can be accomplished using organolithium, Grignard and metal alkoxide reagents.[3a] Thermogravimetric analysis (TGA) combined with UV-Vis–NIR spectroscopy was used to provide a quantitative measure of the degree of functionalisation of the tubes. This degree was found to be roughly one alkyl group for six to eighteen carbon atoms, depending on the nanotubes and the nature of the alkyl group. The alkylated SWCNTs can be well dispersed in common organic solvents.

2.2.2 Addition of Carbenes. Carbene addition is among the first cases of documented sidewall functionalisation. Oxidised SWCNTs were first functionalised with octadecylamine (**14**) followed by addition of phenyl(bromodichloromethyl)-mercury as a source of dichlorocarbene[19] to modify the oxidised tubes (**15**). The reaction course was followed by Raman and IR spectroscopies, and was found to reverse at high temperatures (Scheme 2).

2.2.3 Addition of Nitrenes. The group of Hirsch described the functionalisation of pristine nanotubes by nitrenes, using different alkyl azidoformates as precursors (Scheme 2).[20] After thermally-induced N_2 extrusion, nitrene addition resulted in the formation of alkoxycarbonylaziridino–SWCNT hybrids **16a–g**. This reaction was first applied to small addends (**16a** and **16b**, where R = ethyl and *tert*-butyl, respectively), and then extended to more complex substituents such as long alkyl chains, aromatic groups, crown ethers, dendrimers and oligoethylene glycol units (**16c–g**). The highest solubility of 1.2 mg mL^{-1} was found in dimethylsulfoxide and 1,1,2,2-tetrachloroethane for the SWCNT adducts obtained through the addition of nitrenes bearing crown ethers.

Yinghuai *et al.*[21] reported the covalent sidewall functionalisation of SWCNTs by a substituted C_2B_{10} carborane cage (**17**) *via* a nitrene cycloaddition reaction (Scheme 2). The resulting water soluble nanotubes were administered to tumour-bearing mice and were found to specifically target the tumour. This feature, although not fully explored, could have potential applications for boron neutron capture therapy in cancer treatment.

2.2.4 1,3-Dipolar cycloaddition. The 1,3-dipolar cycloaddition of azomethine ylides generated *in situ* by thermal condensation of aldehydes and α-amino acids produces a large variety of pyrrolidine rings fused to the C–C bonds of SWCNTs.[7a] We have first reported the synthesis of several derivatives containing solubilising alkyl (**18b**) or triethylene glycol chains (**18a**) on the pyrrolidine ring (Scheme 3).[7a] We have also described the covalent linkage of electron donors,

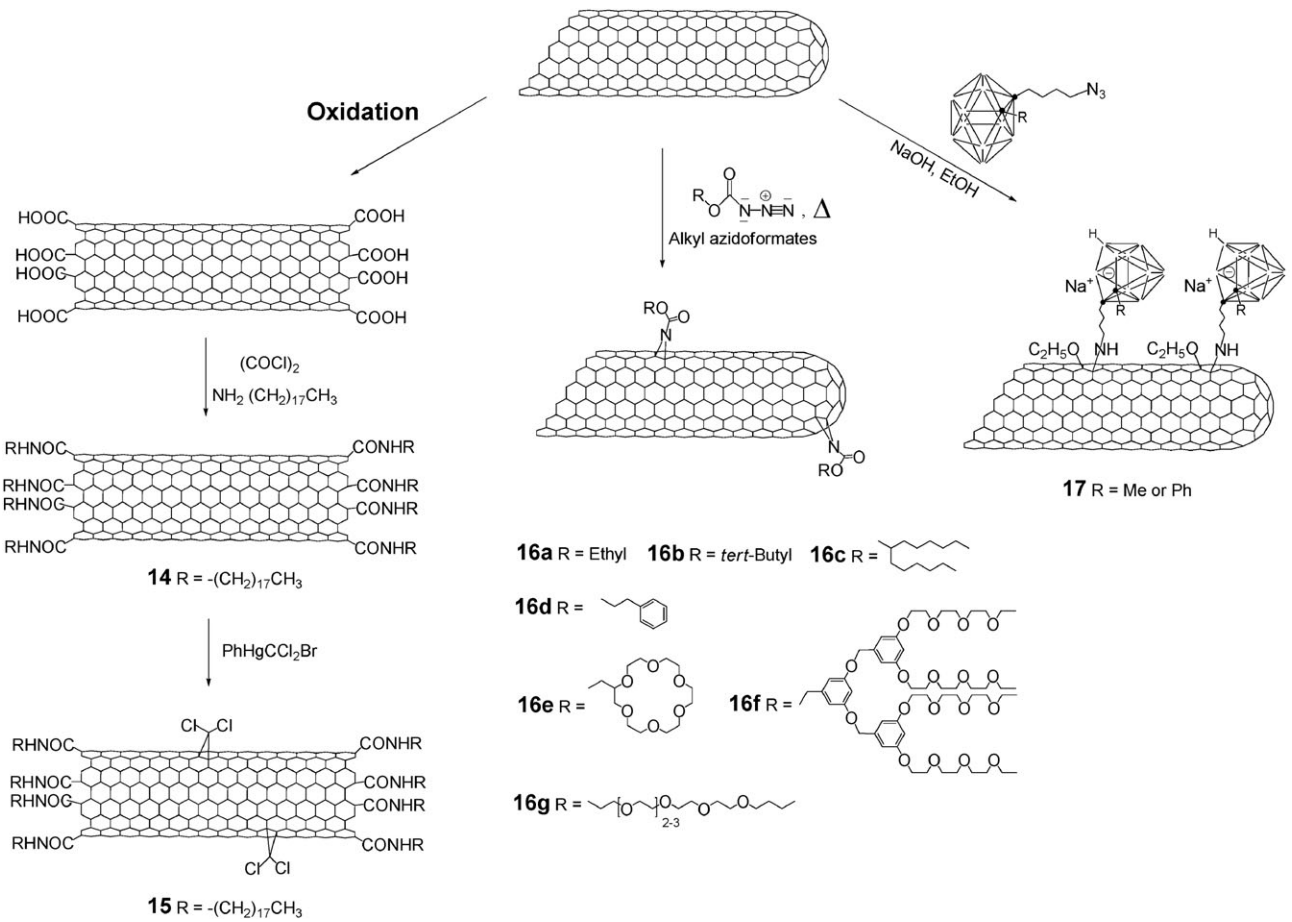

Scheme 2 Carbene and nitrene additions to SWCNTs.

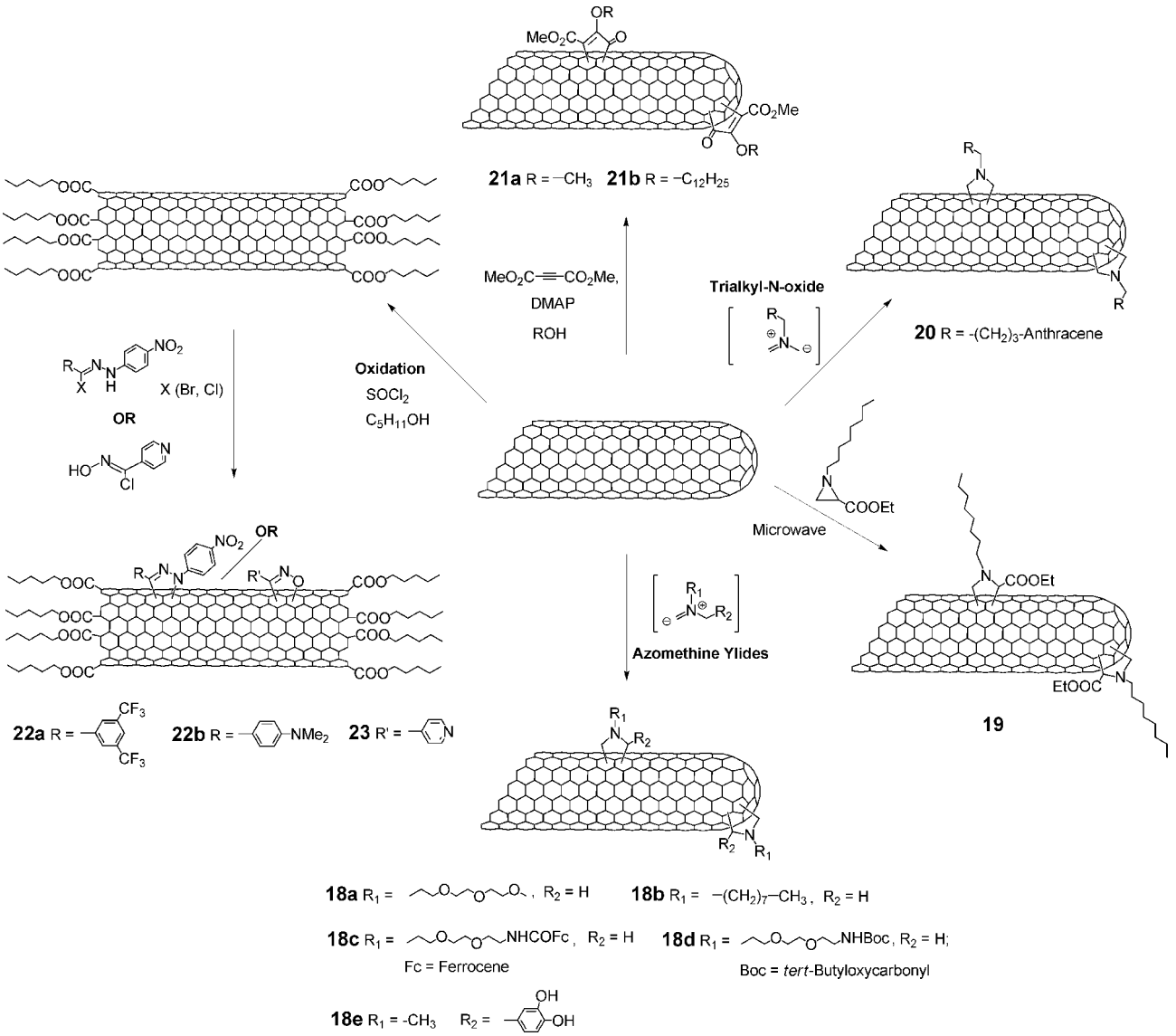

Scheme 3 1,3-Dipolar cycloaddition reactions to SWCNTs.

such as ferrocene (**18c**), onto the network of SWCNTs.[22a] Such types of SWCNT-based conjugates may find application for future developments in photovoltaics. In addition, these ferrocene–nanotube hybrid materials can be used as electrochemical sensors and biosensors for the selective recognition of anions.[22b] The interaction of a large number of ferrocene units with $H_2PO_4^-$ anions in organic solutions, results in a relevant shift of the oxidation potential of the ferrocene unit in cyclic voltammetry experiments.

The use of an *N*-functionalised glycine, bearing a Boc (*tert*-butyloxycarbonyl)-protected amino end group generates the corresponding functionalised SWCNTs (*f*-SWCNTs) (**18d**), which, after deprotection, leads to amine functionalities amenable to further transformations.[23a] Simple procedures in peptide chemistry were then adopted to generate *f*-SWCNTs modified with amino acids and peptides.[23a] These hybrids are attractive tools for biomedical applications.

Recently, SWCNTs functionalised with phenol groups *via* a 1,3-dipolar cycloaddition (**18e**) were described.[23b] Sidewall functionalisation resulted in stable dispersions of SWCNTs in organic and aqueous solvents allowing the preparation of composites. The fabrication of homogenous, coherent and transparent CNT composite films and/or gels was achieved by simple mixing of colloidal suspensions of CNTs with solutions of polymers and layered aluminosilicate clay minerals. We also reported a different approach using microwaves to functionalise SWCNTs employing aziridines as starting materials (**19**).[24] As an indirect proof of functionalisation, retrocycloaddition of SWCNTs has been carried out in the presence of C_{60} to trap the corresponding ylide. Ménard-Moyon *et al.*[25a] reported an alternative method for the functionalisation of SWCNTs by azomethine ylides derived from trialkylamine-*N*-oxides. Selective reaction and separation of semiconducting nanotubes could be achieved when the starting *N*-oxides were attached to pyrene, which acts as a templating agent (**20**).

Zhang and Swager reported the functionalisation of SWCNTs using a zwitterion formed by the reaction of

4-dimethylaminopyridine (DMAP) with dimethyl acetylene dicarboxylate.[25b] The intermediate in this cycloaddition reaction bears positively charged DMAP moieties, which are replaced with a methoxy or 1-dodecanol as the nucleophiles to give **21a–b**. The reaction leads to the formation of cyclopentenyl rings on the nanotubes. Langa and co-workers described the functionalisation of oxidised carbon nanotubes with 2,5-diarylpyrazoline (**22a–b**) or pyridyl–isoxazoline rings (**23**), using 1,3-dipolar cycloaddition of nitrile imines and nitrile oxide, respectively, to the sidewalls of modified SWCNTs.[26] The short nanotubes were first esterified with pentanol and then submitted to cycloaddition, producing **22** and **23**, respectively.

2.2.5 Diels–Alder cycloadditions. In general, 4π + 2π cycloadditions to SWCNTs do not represent a suitable method of functionalisation due to the easy reversibility of this reaction. Langa and co-workers reported the modification of short nanotubes, esterified with pentanol (**24**), by a Diels–Alder cycloaddition (**25**) in the presence of *o*-quinodimethane generated *in situ* from the corresponding 4,5-benzo-1,2-oxathiin-2-oxide (sultine) derivative under microwave irradiation (Scheme 4).[27]

2.2.6 Nucleophilic additions. Coleman *et al.*[28] described the cyclopropanation of SWCNTs (**26a**), using diethyl bromomalonate and 1,8-diazabicyclo[5.4.0]undecene (DBU) (Scheme 5). For the characterisation, they developed a chemical tagging technique, which involves transesterification of the resulting product with 2-(methylthio)ethanol or with the sodium salt of 1*H*,1*H*,2*H*,2*H*-perfluorodecan-1-ol to give **26b** and **26c**, respectively. In the first case, the cyclopropane group was "tagged" by exploiting the gold sulfur binding interaction using preformed 5 nm gold colloidal nanoparticles. In the second case the introduction of perfluoro groups allowed the analysis of the nanotubes by ^{19}F NMR and XPS spectroscopy.

2.2.7 Free-radical additions. This is a widely used class of reactions for SWCNT functionalisation. In general, radicals may form photochemically and/or thermally in oxidation/

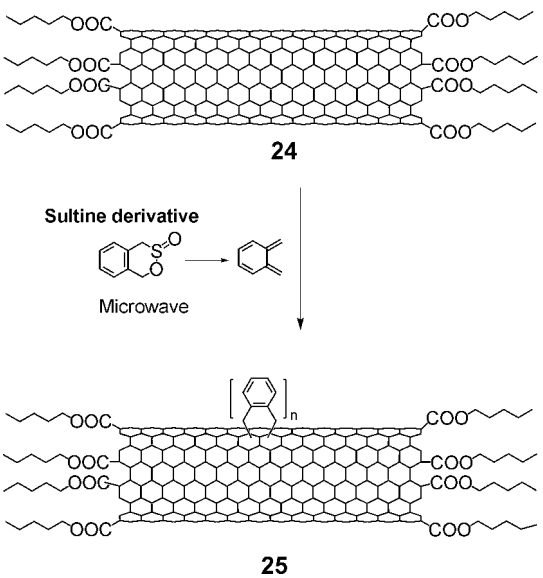

Scheme 4 Diels–Alder cycloaddition reaction to SWCNTs.

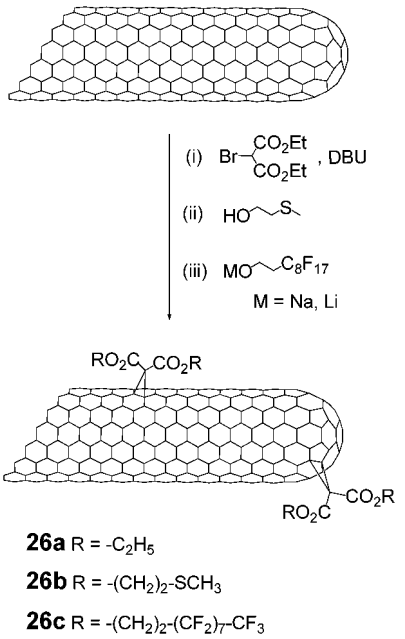

Scheme 5 Nucleophilic addition to SWCNTs.

reduction reactions by inorganic ions, resulting in a single electron transfer, and by electrolysis. Holzinger *et al.*[20a] and Nakamura *et al.*[29] independently reported the addition of perfluorooctyl groups to the surface of nanotubes (**27**). The radicals were generated by photolysis of either heptadecafluorooctyl iodide or perfluoroazooctane (Scheme 6), and they were revealed to covalently react with SWCNTs leading to conjugate **27**. Peng *et al.*[30a] described the reaction of SWCNTs and their fluorinated derivatives with organic peroxides such as benzoyl and lauroyl derivatives under thermal conditions, to produce derivatives **28a** and **28b**. Later, the same group reported the reactions of SWCNTs with succinic or glutaric acyl peroxides resulting in the addition of 2-carboxyethyl or 3-carboxypropyl groups **28c** to the sidewalls of nanotubes. Billups and co-workers reported the reaction of SWCNTs with organic peroxides in the presence of alkyl halides to produce *f*-SWCNTs (**28e–g**).[30b]

Wei and Zhang reported a photoreduction of aromatic ketones by alcohols for covalent sidewall functionalisation.[31a] In this method, benzophenone in the excited state removes a hydrogen atom from benzhydrol, leading to the generation of a benzhydrol radical, which readily adds to the nanotubes. Since the excited benzophenone triplet is reactive to many types of other C–H bonds like amines, ethers, hydrocarbons, or aliphatic sulfides, a wide variety of radicals could be generated using this photochemical approach. A long chain hydrocarbon marker (n-$C_{18}H_{35}$) was grafted onto OH functional groups by an esterification reaction (**29a**). The same authors reported the functionalisation of SWCNTs with diphenylcarbinol groups (**29b**) by the reaction of benzophenone in the presence of potassium.[31b]

2.2.8 Reduction and reductive alkylations. The transformation of nanotubes into carbanionic derivatives is a relatively easy process, owing to their "electron sink" properties. Carbanionic SWCNTs can act as suitable intermediates in a

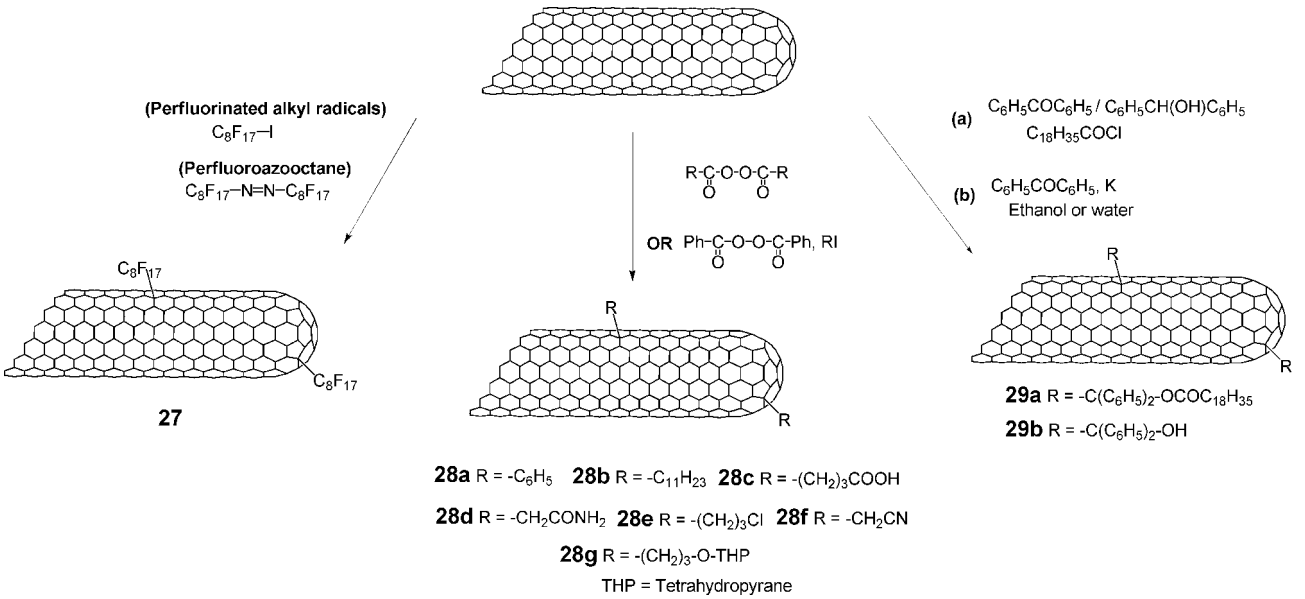

Scheme 6 Functionalisation of SWCNTs using radical additions.

variety of different electrophilic reactions, providing the corresponding functionalised SWCNTs. Pekker *et al.*[32a] first reported the chemical hydrogenation of SWCNTs *via* a Birch reduction with lithium and sodium "electron solvates" $M^+[e^-(NR_3)_n]$ in ethylene diamine or liquid ammonia containing methanol. Similarly, Penicaud *et al.*[32b] showed that mixing alkali metal in THF containing naphthalene results in lithium/sodium naphthalenide radical anion, which could generate carbanionic SWCNTs, easily alkylated with alkyl halides. Liang *et al.*[33] prepared the corresponding alkyl- (**30**) or aryl- (**31**) substituted SWCNTs through a putative reductive alkylation pathway (Scheme 7). The alkylated SWCNTs exhibited high solubility in chloroform, THF and DMF, and also resulted in extensive debundling as observed by AFM and HRTEM characterisations. In the case of arylation, a higher degree of functionalisation was seen when the aryl group was functionalised by an electron donating substituent.

The addition of acrylic ester monomer on nanotube salts (**32a**) was carried out for promoting *in situ* anionic polymerisation onto SWCNTs. The poly(methylmethacrylate)-grafted SWCNTs were soluble in $CHCl_3$, THF and acetone. Similarly, SWCNT salts reacted with ω-bromocarboxylic acids to yield sidewall-derivatised SWCNTs, which could be further coupled to amine-terminated PEG chains to yield water soluble PEGylated SWCNTs (**32b**).[34] The alkyl carbanions (*e.g. sec*-butyl lithium) were added to SWCNTs to generate

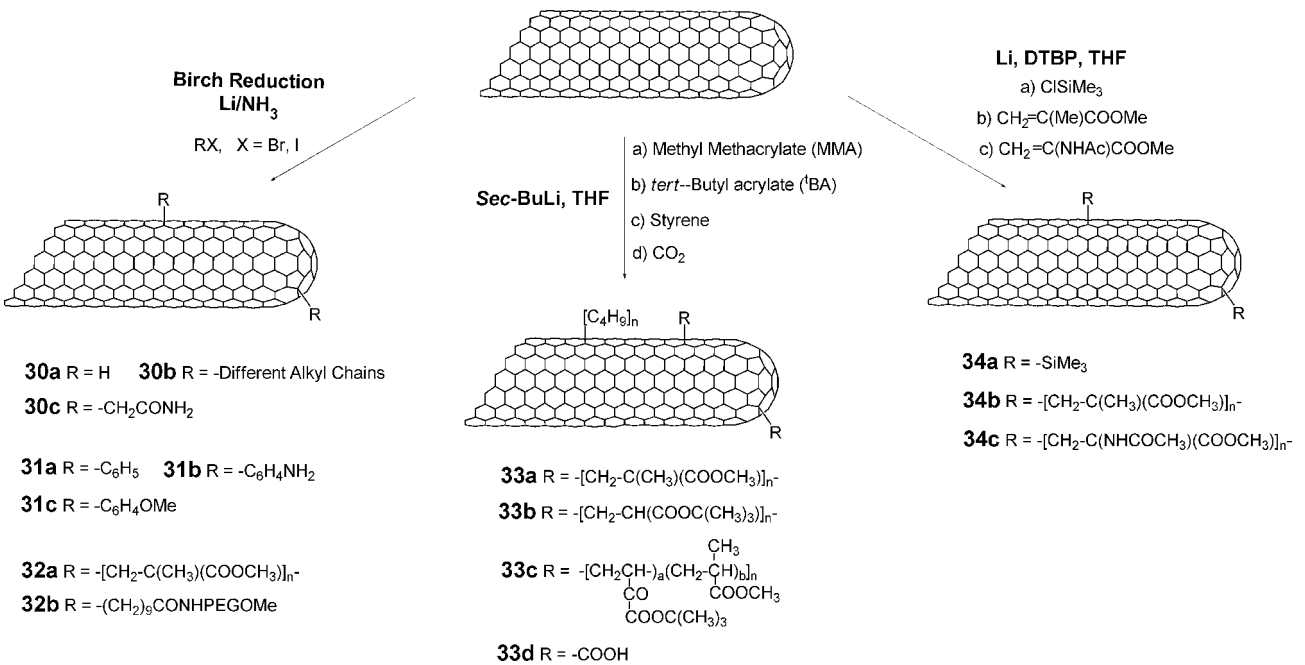

Scheme 7 Functionalisation of SWCNTs using Birch reduction and reductive alkylation, arylation and polymerisation reactions.

anionic sites for grafting polystyrene chains, or to initiate anionic polymerisation of *tert*-butyl acrylate or methyl methacrylate, or block co-polymerisation of these two monomers on the tube surface (**33a–c**). Treating SWCNTs with *sec*-butyllithium, and subsequently with carbon dioxide, led to SWCNTs functionalised with both alkyl and carboxyl groups (**33d**).[35]

In very recently developed methods for generating carbanionic SWCNTs, Garcia-Gallastegui *et al.*[36a] have shown that catalytic amounts of 4,4′-di-*tert*-butyl biphenyl (DTBP) as an electron carrier efficiently promote the formation of carbanionic SWCNTs in THF in the presence of lithium metal. The addition of electrophiles like trimethylchlorosilane, methyl methacrylate and methyl *N*-acetamidoacrylate affords silyl-functionalised nanotubes and polymer wrapped SWCNTs, respectively (**34a–c**). Wunderlich *et al.*[36b] carried out reductive hydrogenation and alkylation of SWCNTs in liquid ammonia by sodium metal in the presence of ethanol–butyl iodide to investigate the SWCNT reaction selectivity. It was found that SWCNTs with smaller diameters were considerably more reactive than tubes with larger diameters. Moreover, this reaction sequence favours the preferred functionalisation of metallic over semiconducting SWCNTs.

2.2.9 Direct arylations. Diazonium coupling is one of the more investigated addition reactions to SWCNTs. Though most probably this reaction proceeds *via* radical intermediates, it is treated apart here because of its importance in the functionalisation panorama. The method was reported by the group of Tour, who described the synthesis of several conjugates (**35**) *via* electrochemical reduction of a variety of preformed aryl diazonium salts, followed by their addition onto the nanotube sidewalls (Scheme 8).[7b] The degree of functionalisation was as high as one functional group out of 20 carbon atoms of SWCNTs. Nanotubes derivatised with a *tert*-butyl benzene moiety were found to possess significantly improved solubility in organic solvents. Later, the same group reported that the functionalisation of SWCNTs with aryl diazonium salts was not only limited to electrochemically induced reactions but could be achieved either by direct treatment with aryl diazonium tetrafluoroborate salts in solution or with the corresponding amine, which was transformed *in situ* into the diazonium species using an alkyl nitrite. In some cases, the reactions with preformed diazonium salts were observed to be effective at moderate or room temperature. It was reported that aryldiazonium salts could efficiently react with SWCNTs

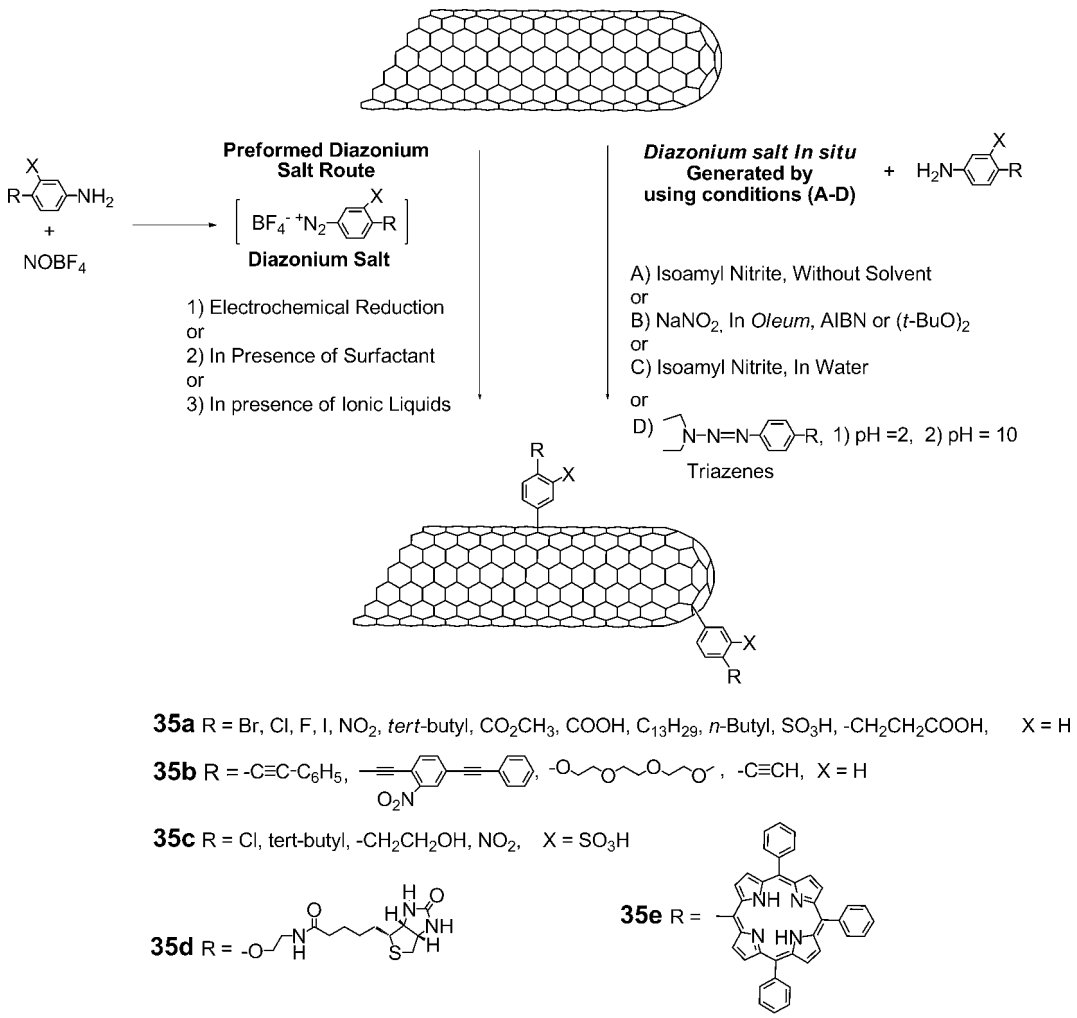

Scheme 8 Functionalisation of SWCNTs using diazonium coupling reactions under different conditions.

coated with sodium dodecyl sulfate (SDS) in water at room temperature.

Dyke and Tour also reported the rapid and green chemical functionalisation of SWCNTs with aryl diazonium salts in the presence of ionic liquids (imidazolium based ionic liquids with various alkyl branched chains) and K_2CO_3 by grinding SWCNT in a pestle and mortar at room temperature for a few minutes.[7b] It is important to note that SWCNTs functionalised in the presence of SDS were more soluble than the aryl-functionalised hybrids prepared by the other methods. For example, SWCNTs containing *tert*-butylphenyl groups exhibited a high solubility in *o*-dichlorobenzene, DMF, chloroform and THF, compared to a low solubility in THF for the solvent-free and electrochemically generated materials, respectively. The Tour group also used organic triazenes as stable precursors to diazonium salts for functionalising SWCNTs in aqueous media (**35d**).[37] A similar approach based on "click chemistry" was explored recently to link a zinc phthalocyanine on SWCNTs pre-functionalised with phenylacetylene moieties.[38] Gho *et al.*[39] reported porphyrin-functionalised SWCNTs by the reaction of nanotubes with *in situ* generated porphyrin diazonium compounds (**35e**). These two examples of nanotubes combined with photoactive species exhibited electron transfer properties by photo-excitation of the phthalocyanine or the porphyrin. The SWCNT–phthalocyanine conjugate **35e** was tested as a photoactive material on an ITO photoanode so that a relatively high incident photon to current efficiency (IPCE) was obtained. In the case of the SWCNT-porphyrin conjugate, the non-linear optical properties were tested: the optical limiting properties were found to be better than those of the separated components (*i.e.* SWCNT and porphyrin), and also than those of fullerene C_{60}. These particular conjugates show that covalently linked donor–acceptors based on nanotubes and porphyrins or phthalocyanines are suitable for the realisation of optoelectronic devices.

3. Characterisation of functionalised carbon nanotubes

Responding to the rapid growth of research in the field of functionalisation of SWCNTs, and the emerging uses in electronics, materials science, nanomedicine and other fields, suitable protocols for SWCNT characterisation to ensure their consistency, structure, purity and reliability have been developed.[40] Due to the unique features of SWCNTs, and the wide range of SWCNTs available from commercial suppliers and academia, characterisation protocols are necessary to help the scientific community to standardise the assessment of SWCNT properties. New techniques have been explored, and existing analytical and spectroscopic methods to characterise the raw, purified and processed (*i.e.* functionalised) SWCNT-based materials have been adapted. The second part of this tutorial review will focus on the available analytical methods for the characterisation of *f*-SWCNTs. The most common techniques that can be employed are reported in Table 1, while some of them are discussed in more detail in the next sections.

Table 1 Different analytical techniques used for the characterisation of *f*-SWCNTs

Analytical techniques[a]		Structural information
Thermal analysis	TGA, DSC, DTA	Purity, thermal stability and degree of functionalisation
Spectroscopy	FTIR	Nature of functional groups
	UV-Vis–NIR	Helicity and degree of functionalisation
	NIR-PL	Helicity of semiconducting tubes
	Raman	Amount of carbon impurities and damage/disorder, degree of functionalisation, diameter and chirality
	XPS	Elemental composition
	AES	Elemental composition
	SIMS	Molecular mass of adsorbate
Microscopy	AFM	Diameter, length
	STM	Helicity and degree of functionalisation
	SEM	Purity
	TEM	Diameter, length, chirality and purity

[a] AES: Auger electron spectroscopy; AFM: atomic force microscopy; DSC: differential scanning calorimetry; DTA: differential thermal analysis; FTIR: Fourier transform infrared; NIR: near infrared; PL: photoluminescence; STM: scanning tunnelling microscopy, SEM: scanning electronic microscopy; SIMS: secondary ion mass spectrometry; TEM: transmission electronic microscopy; TGA: thermal gravimetric analysis; XPS: X-ray photoelectron spectroscopy.

3.1 Thermogravimetric analysis

TGA is an analytical technique used to determine the thermal stability of materials and the fraction of volatile components by monitoring the weight loss that occurs as a sample is heated.[30a,41] The measurement is normally carried out in air or in an inert atmosphere, such as He, N_2 or Ar, and the weight loss is recorded as a function of increasing temperature. Sometimes, the measurements are performed under an oxygen atmosphere (1–5% O_2 in N_2 or He) to enhance the oxidation processes. In addition to the weight changes, some instruments also record the temperature difference between the specimen and one or more reference pans (differential thermal analysis, DTA), or the heat flow into the sample pan compared to that of the reference pan (differential scanning calorimetry, DSC). The latter can be used to monitor the energy released or absorbed *via* chemical reactions during the heating process. In the particular case of *f*-SWCNTs, the weight changes in air are typically a superposition of the weight loss due to oxidation of the organic appendages and the carbon atoms of *f*-SWCNT into gaseous carbon dioxide, while in the case of pristine SWCNTs, an increase in weight can occur due to oxidation of residual metal catalyst into metal oxides. In most cases, TGA is performed with a linear temperature ramp. Typical heating rates employed in TGA measurements of *f*-SWCNT specimens are in the 5–10 °C min^{-1} range. This approach provides two important pieces of information: (i) ash content (residual mass, M_{res}); and (ii) oxidation temperature (T_0). While the definition of ash content is unambiguous, oxidation temperature can be defined in many different ways, including the temperature of the maximum in the weight loss rate (dm/dT_{max}) and the weight loss onset temperature (T_{onset}). The former refers to the temperature of the maximum rate of oxidation, while the latter indicates the temperature when oxidation just begins. The use of the former

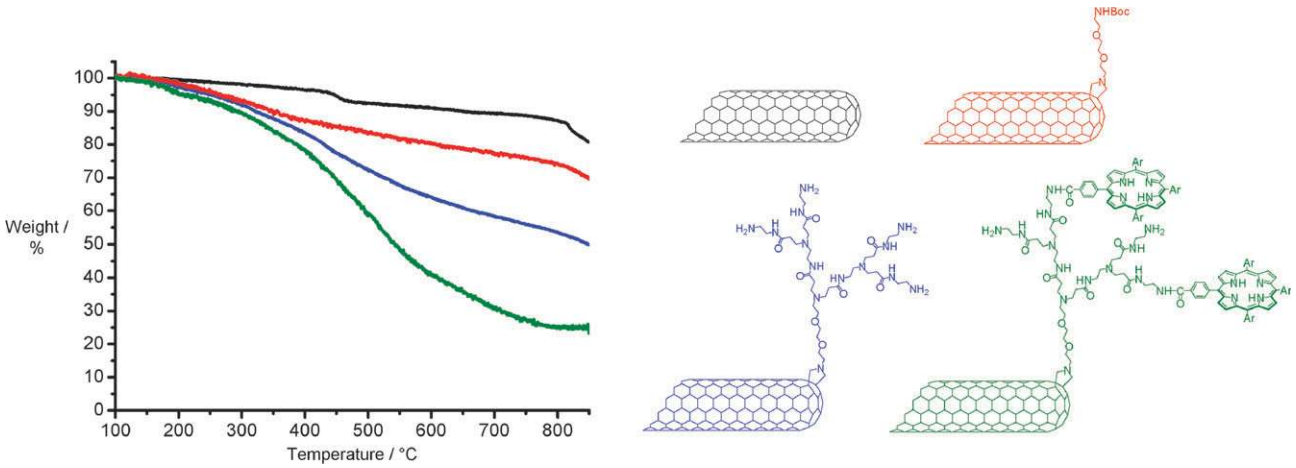

Fig. 1 TGA analysis of pristine SWNTs (black line) and *f*-SWNTs with an increasingly high degree of functionalisation (the red, blue and green lines correspond to the structures on the right). Adapted from ref. 41.

definition, $T_0 = \mathrm{d}m/\mathrm{d}T_{max}$, is preferred, since the precise determination of T_{onset} is often difficult due to the gradual initiation of the thermal transition. However, the gradual onset is essentially attributed to the non-nanotube materials, which burn at temperatures lower than that of SWCNTs, such as the organic residues covalently or physisorbed on the SWCNT sidewalls. Fig. 1 shows an example of thermogravimetric analysis of a series carbon nanotubes functionalised with PAMAM dendrimer and porphyrin.[41] One clearly sees that the loss of weight increases with the increasing degree of functionalisation.

For pristine SWCNTs, the weight loss due to carbon oxidation is often superimposed on the weight increase due to the catalyst oxidation at low temperatures. In some cases, this leads to an upward swing of the TGA curve prior to the bulk of the weight loss, which makes the definition of T_{onset} even more difficult and ambiguous. However, determining $\mathrm{d}m/\mathrm{d}T_{max}$ is relatively straightforward, and herein, the oxidation temperature is defined as $T_0 = \mathrm{d}m/\mathrm{d}T_{max}$. It has been noted that the heating rate has a pronounced effect on the measured values of T_0 and their standard deviations. The effect on T_0 has been attributed to the limited heat conduction into the sample. The maximum temperature is selected so that the specimen weight is stable at the end of the experiment, implying that all chemical reactions are completed.

TGA measurement of *f*-SWCNT-based materials under an inert atmosphere usually produces only one peak in the $\mathrm{d}m/\mathrm{d}T$ curve, as the organic functionalisation decomposes rapidly and more effectively than the carbon framework. Sometimes, more than one peak is observed, due to the difference in thermal stability of parts of the appended fragments. These partially overlapped peaks can be deconvoluted, allowing quantification of the various components in the nanotube material (amorphous carbon, tubes, or graphitic particles).

It is not surprising that when TGA measurements are performed on several SWCNT-containing specimens sampled from the same batch, the TGA traces do not necessarily coincide. These observations serve to emphasize that SWCNT batches are not pure chemicals and, therefore, are not as homogenous and uniform as usually implied for pure classical molecules. This supports the idea that there is always some variation that exceeds the accuracy and reproducibility of the instrumental measurements. This means that values of M_r and T_0 produced in one TGA run are not necessarily representative of the whole batch. The only reasonable approach to overcome this problem is to perform TGA on at least three (or more) specimens sampled from the same batch and calculate mean averages of M_r and T_0 with their standard deviations (σM_r and σT_0). It is obvious that the latter values can serve as a measure of the structural inhomogeneity of the nanotubes within the batch.

3.2 Spectroscopic characterisations

3.2.1 Resonantly enhanced Raman spectroscopy. Raman measurements explicitly involve phonons, independently on the electronic structure of the material and the laser energy used to excite it.[42a,43a] The usual Raman scattering signal is weak. However, its intensity can be improved when the laser energy matches the energy between optically allowed electronic transitions in the material studied. This enhancement of the intensity is called resonance Raman scattering. In 1D system like SWCNTs, the characteristic van Hove singularities (vHS) define narrow energy ranges where the intensity of the electronic density of state (DOS) becomes very large. In practice, a single SWCNT exhibits a "molecular-like" behaviour, with well-defined electronic energy levels at each vHS. The resonance Raman signal from a SWCNT can be obtained when the laser excitation energy is equal to the energy separation between the vHS in the valence and conduction bands, but restricted to the selection rules for optically allowed electronic transitions. The two most prominent features observed in the first-order resonant Raman spectrum of SWCNTs are the low-frequency radial breathing mode (RBM, between 100–300 cm^{-1}) and the high frequency tangential mode (*i.e.* the G band, between 1500–1600 cm^{-1}). The Raman-allowed tangential mode in graphite is observed at 1582 cm^{-1} and is called the G mode, as defined from graphite. Unlike graphite, the tangential G mode in SWCNTs gives rise to a multi-peak feature where up

to six Raman peaks can in principle be observed. However, common analyses are carried out considering the two most intense peaks, which basically originate from the symmetry breaking of the tangential vibration when the graphene sheet is rolled to make a cylindrically shaped tube. The two most intense G peaks are labelled G^+, for atomic displacements along the tube axis, and G^-, for modes with atomic displacement along the circumferential direction. The lowering of the frequency for the G^- mode is caused by the curvature of the nanotube framework, which is often the tangential vibration in the circumferential direction. The difference between the G band line shape for semiconducting and metallic SWCNTs is evident in the case of the G^- band, which is broadened for metallic SWCNTs in comparison with the Lorentzian-like line shape for semiconducting tubes.[43b] This broadening is related to the presence of free electrons in nanotubes with metallic character. Due to the resonant nature of the SWCNT Raman response, multiple excitation wavelengths must be used to allow for the contributions of SWCNTs of different diameters.

Another important feature in the Raman spectra is the low-intensity dispersive D band (diamond band, or disorder band), which is typically located in the 1200–1400 cm^{-1} region. The peak position of the band shifts to higher wavenumbers as the laser excitation energy (E_{laser}) is increased. This band is associated with disorder, specifically, the sp^3-hybridised carbon atoms present on the SWCNT sidewall or as other carbon species in the carbonaceous impurities. In particular, the occurrence and the magnitude of such D bands, are used to indicate the presence and extent of functionalisation in *f*-SWCNTs. Therefore, the D band also represents the change of C atoms from an sp^2 to an sp^3 hybridisation state, which breaks the symmetry of the graphite plane.

Other spectral features, in the RBM and G modes (excluding the D-band) originating from either a double-resonance process or from folding the phonon dispersion of 2D graphite into a 1D Brillouin zone, can also be observed. Most of the peaks are so weak that they must be viewed on an expanded scale to appear clearly in the spectra, and the physics needed to understand their behaviour is also more sophisticated. These peaks are essentially interesting for the structural and electronic SWCNT characterisation, first because they give information about many phonon branches, important for the transport, thermal and mechanical properties of carbon nanotubes, and second, because they exhibit chirality-dependent frequencies (as they come from the anisotropic 2D phonon Brillouin zone).[42a]

Functionalisation of SWCNTs affects the intensity of the Raman bands. First, the intensity of the D-band increases relative to that of the G-band. Raman studies on SWCNTs functionalised through many methodologies have shown that the intensity ratio between the D band and the G band increases with the reaction extent. It has been demonstrated that the intensity of the D band can easily exceed that of the G band after covalent coupling of phenyl radicals to individual SWCNTs with a functionalisation degree of 10% or higher.[42b] In addition, covalently functionalised SWCNTs exhibit reduced intensities of the RBM and the G band, as compared to the unmodified tubes. The RBM completely disappears for high functionalisation degrees, while the separate tangential modes within the G band develop into one very broad, but still detectable peak at 1590 cm^{-1}, the same frequency at which the in-plane E_{2g} stretching vibration appears in the Raman spectrum of graphitic materials.

As an example, let us take into consideration the series of reactions shown in Scheme 9. On a SWCNT, a 1,3-dipolar cycloaddition is first performed, followed by a direct arylation reaction.[44]

The combination of these two reactions in sequence, achieved using microwave activation, gives rise to a valuable multiple functionalisation, which can be efficiently followed

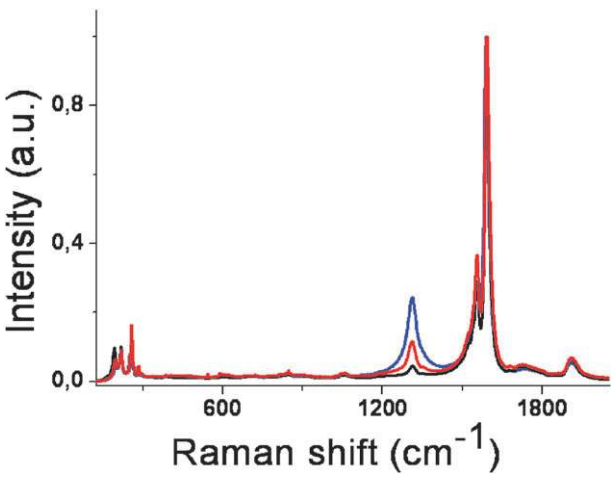

Fig. 2 Raman spectra (λ_{exc} = 632.8 nm) of pristine SWCNTs (black line), cycloadduct **36** (red line) and adduct **37** (blue line).

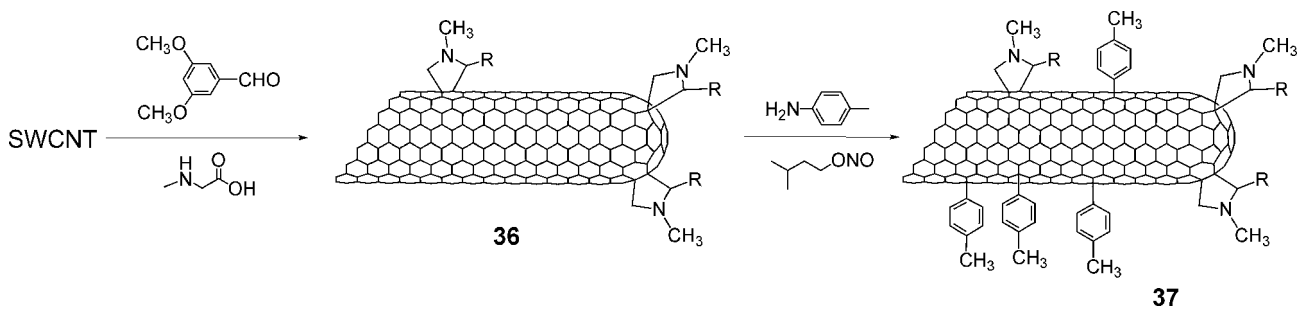

Scheme 9 Double functionalisation of SWCNT: 1,3-dipolar cycloaddition followed by direct arylation.[44]

using Raman spectroscopy. Fig. 2 reports the Raman spectra of the pristine starting material, cycloadduct **36** and the product of arylation **37**.

Notably, the relative intensity of the D band strongly increases as the degree of functionalisation increases. The intensity of the D band reveals that the arylation reaction further increases the functionalisation degree after the cycloaddition has occurred. Even though a quantitative relationship between the intensity of the D band and the degree of functionalisation cannot be concluded, the relative intensity of the D band in relation to the G band gives a rough estimate of the extent of functionalisation.

3.2.2 UV-Vis–NIR absorption spectroscopy. The optical absorption spectra in the UV-Vis–NIR range of pristine SWCNTs show characteristic absorptions due to the transitions between the first and second pairs of singularities in the density of states of the tubes.[45] Each (n,m) carbon nanotube exhibits a different set of van Hove singularities in its valence and conduction bands; therefore, optical absorption can be used to determine the chirality of the nanotubes.

Bundled tubes show broad optical absorption peaks (black line in Fig. 3). The electronic structure evaluation of SWCNTs has greatly benefited from a recently developed method to isolate individual nanotubes within surfactants, with sharp optical absorption peaks (blue line in Fig. 3).[46]

Covalent modification of SWCNTs induces changes in the electronic structure that can be probed by optical absorption spectroscopy. With an increasing degree of functionalisation, the π-conjugation is increasingly deteriorated. At low densities of attached groups, the S_{11}, S_{22} and M_{11} transitions can still be discerned in the UV-Vis–NIR spectrum (with diminished intensity). Such behaviour has, for instance, been reported for oxidised SWCNTs,[46] or for SWCNTs modified by the addition of nitrenes.[20b] At higher functionalisation degrees, a complete loss of the S_{11}, S_{22} and M_{11} features is observed, as documented for the addition of various types of organic residues to carbon nanotubes.[30a]

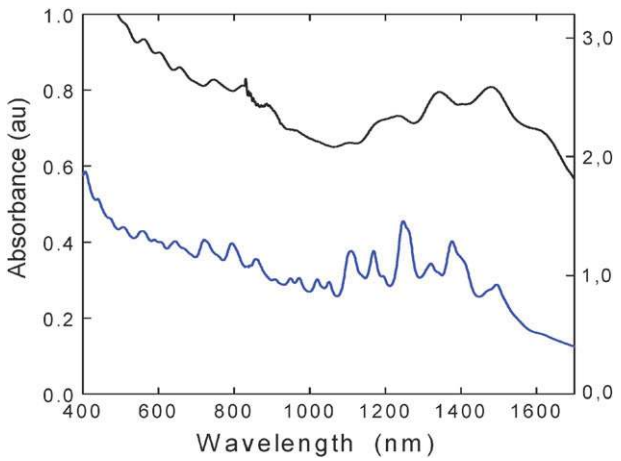

Fig. 3 Vis–NIR absorption spectra of individual (blue line) and bundled (black line) SWCNTs. Vis–NIR absorption spectra of SWCNTs in SDS–D_2O suspension. The top trace (black line) is typical of tubes prepared in suspension without centrifugation. The broadened and red-shifted absorption features show that most nanotubes in the sample are aggregated in small bundles. The bottom trace (blue line) is from samples of individual nanotubes separated and solubilised in SDS micelles. Adapted from ref. 46.

3.2.3 Infrared spectroscopy. Infrared spectroscopy gives much less information about the vibrational properties of carbon nanotubes compared to Raman spectroscopy, mostly due to the strong absorption of SWCNTs in the IR range.[42a] The main active modes for carbon nanotubes are the A_{2u} and E_{1u} modes, observed at around 874 and 1598 cm^{-1} for SWCNTs. The number of infrared-active phonon modes depends on the chiral indices. Armchair, zig-zag and chiral tubes have, respectively, three, three, and six IR-active modes. IR spectroscopy is often used to characterise impurities from synthesis or to identify functional groups of molecules covalently attached to the nanotube surface.[42a] In particular, IR is useful to characterise oxidised nanotubes. Indeed, purification and/or oxidation of carbon nanotubes introduces carbonyl and carboxylic groups, which are easily visualised due to the C=O stretching band around 1700 cm^{-1}.[47a] This band usually shifts towards a smaller wavenumber (below 1700 cm^{-1}) after the functionalisation of the carboxylic groups with amines.[9,19] Therefore, a careful examination of the band positions can give precious indications of the reaction. In addition to the C=O stretching band, other peaks can be useful for the characterisation and, notably, the band corresponding to the C–H vibration between 2800 and 3000 cm^{-1}. These series of peaks are normally absent in non-functionalised nanotubes and appear with the incorporation of organic fragments onto the nanotubes. Other peaks can be attributed to particular functions and covalent bonds like C–F (~1100 and 1250 cm^{-1}),[47b] C–Cl (~798 cm^{-1})[19] or O–H (~3200–3500 cm^{-1}).[47a]

3.2.4 Emission spectroscopy. Weisman *et al.* observed that individual semiconducting SWCNTs emit band-gap photoluminescence (PL) in the near-infrared.[46] They have reported distinct electronic absorption and emission transitions for more than 30 semiconducting nanotubes. The emission peaks are red-shifted by ~40 cm^{-1} with respect to the corresponding absorption bands, which implies that there are only minor geometrical changes upon optical excitation. The quantum yield of SWCNTs has been reported as high as 10^{-3} and their lifetimes are in the low picosecond range.[46,48] The E_{11} and E_{22} optical transitions have been assigned to specific tube chiralities (n,m),[48,49] thus demonstrating how fluorescence is a valuable analytical method for identifying the structures of individual SWCNTs. Fig. 4 shows the fluorescence map of SWCNTs dispersed in *N*-methyl-2-pyrrolidone (NMP). Each peak corresponds to a single (n,m) SWCNT. The red circles on the map indicate PL maxima of nanotubes dispersed in sodium dodecylbenzene sulfonate (SDBS) surfactant. The assignment of PL peaks to specific (n,m) nanotubes is in accordance with Bachilo *et al.*[49]

Big bundles of nanotubes do not emit. The metallic tubes present in the bundles strongly quench the emission of the semiconducting tubes, thus providing useful evidence for measuring SWCNT dispersion.[50] However, Tan *et al.*[51] have recently showed that it is possible to detect and interpret the

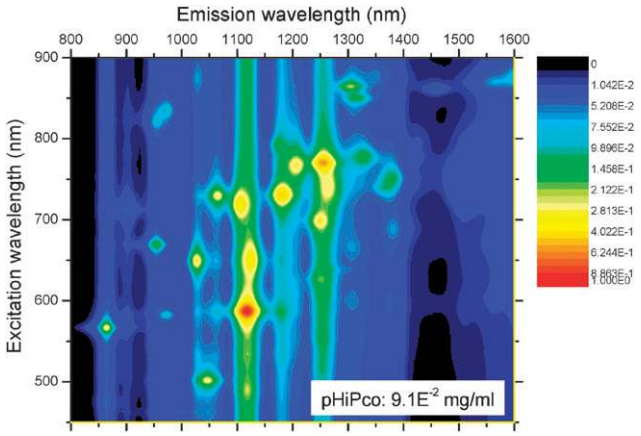

Fig. 4 Photoluminescence map of commercially available pristine SWCNTs (HiPco) dispersed in SDBS aqueous solutions.

PL of carbon nanotubes in bundles by considering the exciton energy transfer between tubes. The emission is also strongly suppressed after chemical functionalisation of SWCNTs. Cognet *et al.*[50] reported reversible stepwise quenching of individual SWCNTs by acid and irreversible quenching of individual SWCNT exposed to diazonium salts.

3.2.5 Nuclear magnetic resonance spectroscopy. Nuclear magnetic resonance (NMR) is a very important tool for the structural assignment of organic substances. However, in the case of functionalised SWCNTs, the proton signals in the organic addends appear broad as a result of the statistical distribution of the addends on the SWCNT surface.[52] Furthermore, interactions between the protons of the functional groups and the π system of SWCNTs, the non-negligible content of traces of catalytic metal impurities, as well as the restricted mobility of SWCNTs in solution due to their large size, contribute to line-broadened signals. Thus far, both proton and carbon NMR spectroscopy in solution does not represent a suitable way for functionalisation detection and characterisation of SWCNTs.

3.3 Scanning probe microscopy

All scanning probe microscopy techniques involve scanning action of an extremely sharp tip (3–50 nm radius of curvature) across the surface of an object. The tip is mounted on a flexible cantilever, allowing the tip to follow the surface profile. When the tip moves in proximity of the investigated object, the interactions between the tip and the surface influence the movement of the cantilever. These movements are detected by selective sensors. Various interactions can be studied depending on the mechanics and working principle of the probe. The two most common scanning techniques used to characterise functionalised SWCNTs are atomic force microscopy (AFM) and scanning tunneling microscopy (STM). AFM measures the interaction forces between the tip and the surface, while the tip is dragged across the surface or it vibrates as it moves. STM measures the tunneling current flowing between the tip and the sample at a fixed distance. Surface imaging provides valuable nanoscale information. They often have atomic resolution and can also give spectroscopic information at the nanoscale level.[53]

3.3.1 Atomic force microscopy. AFM is an invaluable tool for the morphological visualisation of carbon nanotubes in the bulk and to measure their size distribution (diameters and lengths). AFM measurements on deposited films, usually obtained from spin-coated dispersions of SWCNTs in NMP at different concentrations, reveal that the bundle diameter distribution decreases dramatically with decreasing concentration.[54] Photoluminescence studies over the same concentration range confirmed that the AFM measurements reflect the diameter distributions *in situ*.[54] Fig. 5 shows a representative image for nanotubes at concentrations of 1 μg ml^{-1}. The line sections show the presence of objects of diameter ~1 nm, corresponding to individual nanotubes. It should be pointed out that reliable length distributions of pristine nanotubes at high concentration are difficult to obtain using AFM, as completely isolated objects are rare and it can be difficult to determine the positions of the ends of a given bundle. In these cases it might be preferable to measure the bundle length by TEM.

AFM was also used to identify selenium nanoparticles adsorbed on polar functional groups, introduced by an oxidative process,[55] to identify gold nanoparticles adsorbed on sulfur-containing substituents,[56] and therefore to indirectly monitor the functionalisation sites. However, the use of nanoparticles as chemical markers for AFM could give misleading results for substituent distribution, as proven with STM studies.[57] AFM can also be used to distinguish SWCNTs from other types of tubes like double-walled CNTs, as distinct mechanical signatures can be measured.[58]

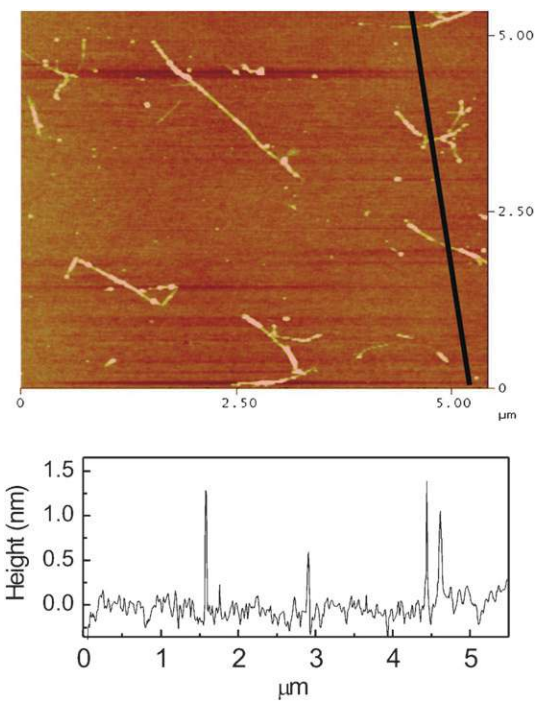

Fig. 5 Typical AFM image of a 1 μg ml^{-1} dispersion of purified SWCNTs (from HiPco dispersed in NMP) and spin-coated on mica.

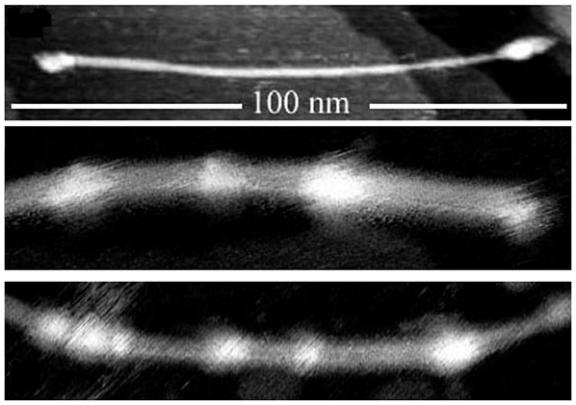

Fig. 6 STM images of SWCNTs functionalised with octadecylamine. Adapted from ref. 60.

3.3.2 Scanning tunnelling microscopy. The groups of Lieber and Dekker used STM to directly reveal the real-space atomic structures of SWCNTs with various chiralities.[59,60] They obtained hexagonal lattice images of SWCNTs and (n,m) indices from the experimentally measured values of the chiral angle and diameter. Scanning tunnelling microscopy and spectroscopy (STS) can thus simultaneously correlate atomic structures with the electronic properties of the nanotubes.

STM is also a versatile technique for imaging organic functional groups covalently attached to the nanotubes, and has been reported for fluorinated SWCNTs, for SWCNTs functionalised *via* a Bingel reaction, and for thiol- and thiophene-functionalised SWCNTs.[57] Our STM studies on short SWCNTs functionalised with octylamine and octadecylamine has unambiguously shown the presence of aliphatic moieties attached predominantly at the tips of the oxidised nanotubes.[61] Fig. 6 shows the STM images of SWCNTs functionalised with octadecylamine groups.

3.4 Electron microscopy

3.4.1 Transmission electron microscopy. Transmission electron microscopy (TEM) is a major tool for the morphological visualisation of SWCNTs in bulk, the measurement of their lengths and diameters, and a crude assessment of their purity. In addition, high resolution TEM (HRTEM) can provide images with atomic resolution. With the development of HRTEM techniques, direct imaging of chiral structures of nanotubes have been achieved in addition to diffraction studies.[62,63] The spatial resolution for conventional HRTEM has been recently improved, allowing the visualisation of hexagonal lattices in graphene sheets. The fine electron beam available in modern transmission electron microscopes offers a unique probe for revealing the atomic structure of individual nanotubes. In a recent review Qin has shown that electron diffraction patterns could provide an accurate and unambiguous assignment of the chiral indices of SWCNTs.[64] The chiral indices can be read with a high accuracy from the intensity distribution on the principal layer lines in an electron diffraction pattern.[64,65]

Hirahara *et al*. recently reported the first 3D-like aberration-corrected HRTEM imaging of SWCNTs.[66] Very recently a single small organic molecule inside a SWCNT was observed with near-atomic resolution by TEM.[67]

3.4.2 Scanning electron microscopy. Scanning electron microscopy (SEM) has been widely used to visualise SWCNTs in the bulk and to assess their purity. Unfortunately, SEM provides limited information on the presence of functional groups due to its relatively low magnification. The spot size and the interaction volume are very large compared to the atomic distances, and SEM cannot provide images with atomic resolution. In contrast, of particular interest are Z-contrast scanning transmission electron microscopic (STEM) techniques, which allow the detection of a mass thickness contrast, resulting in higher intensities in correspondence of thicker regions and/or heavier elements. With this technique, we were able to detect and prove the presence of high Z element agglomerates onto the bundle surface of SWCNTs coated with Eu(III)-containing complexes.[68]

4. Conclusions

The functionalisation of SWCNTs covers a wide variety of organic reactions. Some of them are very efficient in affording highly functionalised and relatively soluble nanotubes. As a consequence, SWCNTs can be manipulated and used in a range of applications covering the fields of materials science and nanomedicine. Since functionalised SWCNTs are complex structures, several techniques have been adapted for their characterisation. It is of fundamental importance to combine different spectroscopic and microscopic methods to prove the presence of the functional groups around the tips and the sidewalls of the nanotubes, and to quantify these groups along with the impurity content. More and more SWCNT conjugates continue to emerge for future technologies, both in materials and life sciences, making functionalisation of SWCNTs a very fascinating and exciting research field.

Acknowledgements

We gratefully acknowledge the generous financial support by the European Union (through the Marie-Curie Research Training Network PRAIRIES, contract MRTN-CT-2006-035810, Initial Training Network FINELUMEN, PITN-GA-2008-215399, NEURONANO program NMP4-CT-2006-031847), INSTM, MIUR (COFIN prot. 2006034372 and FIRB RBIN04HC3S), the "Agence National de la Recherche" (ANR-05-JCJC-0031-01), Science Foundation Ireland (PIYRA 07/YI2/I1052), the Belgian National Research Foundation (FRS-FNRS) and "Loterie Nationale" (through the contracts no. 2.4.625.08 and 2.4.550.09) and the University of Namur. A.B. and P.S. wish to thank the support of the French-Indian CEFIPRA collaborative project (Project no. 3705-2).

References

1 (*a*) M. Monthioux and V. L. Kuznetsov, *Carbon*, 2006, **44**, 1621; (*b*) S. Iijima, *Nature*, 1991, **354**, 56.
2 (*a*) S. Iijima and T. Ichihashi, *Nature*, 1993, **363**, 603; (*b*) D. S. Bethune, C. H. Klang and M. S. de Vries, *Nature*, 1993, **363**, 605.

3 (*a*) See articles in *Acc. Chem. Res.*, 2002, **35**, 997–1113, special issue on "Carbon Nanotubes", ed. R. C. Haddon; (*b*) C. N. R. Rao, B. C. Satishkumar, A. Govindaraj and M. Nath, *ChemPhysChem*, 2001, **2**, 78.
4 (*a*) A. Jorio, G. Dresselhaus and M. S. Dresselhaus, *Carbon Nanotubes: Advanced Topics in the Synthesis, Structure, Properties and Applications*, Springer-Verlag, Berlin, Heidelberg, 2008; (*b*) S. Reich, C. Thomsen and J. Maultzsch, *Carbon Nanotubes: Basic Concepts and Physical Properties*, Wiley-VCH, Weinheim, Germany, 2004.
5 (*a*) F. Kreupl, *Carbon Nanotubes in Microelectronic Applications*, Wiley-VCH, Verlag GmbH & Co. KgaA, Weinheim, 2008; (*b*) F. Cataldo and T. Da Ros, *Medicinal Chemistry and Pharmacological Potential of Fullerenes and Carbon Nanotubes*, Springer-Verlag, Berlin, Heidelberg, 2008.
6 J. Liu, A. G. Rinzler, H. Dai, J. H. Hafner, R. K. Bradley, P. J. Boul, A. Lu, T. Iverson, K. Shelimov, C. B. Huffman, F. Rodriguez-Marcias, Y.-S. Shon, T. R. Lee, D. T. Colbert and R. E. Smalley, *Science*, 1998, **280**, 1253.
7 (*a*) D. Tasis, N. Tagmatarchis, A. Bianco and M. Prato, *Chem. Rev.*, 2006, **106**, 1105; (*b*) C. A. Dyke and J. M. Tour, *J. Phys. Chem. B*, 2004, **108**, 11151.
8 (*a*) M. A. Hamon, J. Chen, H. Hu, Y. Chen, M. E. Itkis, A. M. Rao, P. C. Eklund and R. C. Haddon, *Adv. Mater.*, 1999, **11**, 834; (*b*) B. Zhao, H. Hu and R. C. Haddon, *Adv. Funct. Mater.*, 2004, **14**, 71.
9 F. Pompeo and D. E. Resasco, *Nano Lett.*, 2002, **2**, 369.
10 (*a*) J. L. Delgado, P. de la Cruz, A. Urbina, J. T. L. Navarrete, J. Casado and F. Langa, *Carbon*, 2007, **45**, 2250; (*b*) W. Wu, H. Zhu, L. Fan and S. Yang, *Chem.–Eur. J.*, 2008, **14**, 5981.
11 S. Giordani, J.-F. Colomer, F. Cattaruzza, J. Alfonsi, M. Meneghetti, M. Prato and D. Bonifazi, *Carbon*, 2009, **47**, 578.
12 E. Katz and I. Willner, *ChemPhysChem*, 2004, **5**, 1084.
13 (*a*) P. He and M. W. Urban, *Biomacromolecules*, 2005, **6**, 2455; (*b*) S. E. Baker, W. Cai, T. L. Lasseter, K. P. Weidkamp and R. J. Hammers, *Nano Lett.*, 2002, **2**, 1413.
14 (*a*) L. Gu, T. Elkin, X. Jiang, H. Li, Y. Lin, L. Qu, T.-R. J. Tzeng, R. Joseph and Y.-P. Sun, *Chem. Commun.*, 2005, 874; (*b*) S.-Y. Ju and F. Papadimitrakopoulos, *J. Am. Chem. Soc.*, 2008, **130**, 655.
15 (*a*) L. Sheeney-Haj-Ichia, B. Basnar and I. Willner, *Angew. Chem., Int. Ed.*, 2005, **44**, 78; (*b*) F. Patolsky, Y. Weizmann and I. Willner, *Angew. Chem., Int. Ed.*, 2004, **43**, 2113.
16 (*a*) H. Li, R. B. Martin, B. A. Harruff, R. A. Carino, L. F. Allard and Y.-P. Sun, *Adv. Mater.*, 2004, **16**, 896; (*b*) D. Baskaran, J. W. Mays, X. P. Zhang and M. S. Bratcher, *J. Am. Chem. Soc.*, 2005, **127**, 6916.
17 S. Cosnier and M. Holzinger, *Electrochim. Acta*, 2008, **53**, 3948.
18 (*a*) D. Srivastava, D. W. Brenner, J. D. Schall, K. D. Ausman, M. Yu and R. S. Ruoff, *J. Phys. Chem. B*, 1999, **103**, 4330; (*b*) E. T. Mickelson, C. B. Huffman, A. G. Rinzler, R. E. Smalley, R. H. Hauge and J. L. Margrave, *Chem. Phys. Lett.*, 1998, **296**, 188.
19 H. Hu, B. Zhao, M. A. Hamon, K. Kamaras, M. E. Itkis and R. C. Haddon, *J. Am. Chem. Soc.*, 2003, **125**, 14893.
20 (*a*) M. Holzinger, O. Vostrowsky, A. Hirsch, F. Hennrich, M. Kappes, R. Weiss and F. Jellen, *Angew. Chem., Int. Ed.*, 2001, **40**, 4002; (*b*) M. Holzinger, J. Abraham, P. Whelan, R. Graupner, L. Ley, F. Hennrich, M. Kappes and A. Hirsch, *J. Am. Chem. Soc.*, 2003, **125**, 8566.
21 Z. Yinghuai, A. T. Peng, K. Carpenter, J. A. Maguire, N. S. Hosmane and M. Takagaki, *J. Am. Chem. Soc.*, 2005, **127**, 9875.
22 (*a*) D. M. Guldi, M. Marcaccio, D. Paolucci, F. Paolucci, N. Tagmatarchis, D. Tasis, E. Vázquez and M. Prato, *Angew. Chem., Int. Ed.*, 2003, **42**, 4206; (*b*) A. Callegari, M. Marcaccio, D. Paolucci, F. Paolucci, N. Tagmatarchis, D. Tasis, E. Vázquez and M. Prato, *Chem. Commun.*, 2003, 2576.
23 (*a*) M. Prato, K. Kostarelos and A. Bianco, *Acc. Chem. Res.*, 2008, **41**, 60; (*b*) V. Georgakilas, A. Bourlinos, D. Gournis, T. Tsoufis, C. Trapalis, A. Mateo-Alonso and M. Prato, *J. Am. Chem. Soc.*, 2008, **130**, 8733.
24 F. G. Brunetti, M. A. Herrero, Juan de M. Munoz, S. Giordani, A. Diaz-Ortiz, S. Filippone, G. Ruaro, M. Meneghetti, M. Prato and E. Vazquez, *J. Am. Chem. Soc.*, 2007, **129**, 14580.
25 (*a*) C. Ménard-Moyon, N. Izard, E. Doris and C. Mioskowski, *J. Am. Chem. Soc.*, 2006, **128**, 6552; (*b*) W. Zhang and T. M. Swager, *J. Am. Chem. Soc.*, 2007, **129**, 7714.
26 M. Alvaro, P. Atienzar, P. de la Cruz, J. L. Delgado, V. Troiani, H. Garcia, F. Langa, A. Palkar and L. Echegoyen, *J. Am. Chem. Soc.*, 2006, **128**, 6626 and references therein.
27 J. L. Delgado, P. de la Cruz, F. Langa, A. Urbina, J. Casado and J. T. López Navarrete, *Chem. Commun.*, 2004, 1734.
28 K. S. Coleman, S. R. Bailey, S. Fogden and M. L. H. Green, *J. Am. Chem. Soc.*, 2003, **125**, 8722.
29 T. Nakamura, M. Ishihara, T. Ohana, A. Tanaka and Y. Koga, *Chem. Commun.*, 2004, 1336.
30 (*a*) H. Peng, L. B. Alemany, J. L. Margrave and V. N. Khabashesku, *J. Am. Chem. Soc.*, 2003, **125**, 15174 and references therein; (*b*) Y. Ying, R. K. Saini, F. Liang, A. K. Sadana and W. E. Billups, *Org. Lett.*, 2003, **5**, 1471.
31 (*a*) L. Wei and Y. Zhang, *Nanotechnology*, 2007, **18**, 495703; (*b*) L. Wei and Y. Zhang, *Chem. Phys. Lett.*, 2007, **446**, 142.
32 (*a*) S. Pekker, J.-P. Salvetat, E. Jakab, J.-M. Bonard and L. Forro, *J. Phys. Chem. B*, 2001, **105**, 7938; (*b*) A. Penicaud, P. Poulin, A. Derre, E. Anglaret and P. Petit, *J. Am. Chem. Soc.*, 2005, **127**, 8.
33 F. Liang, A. K. Sadana, A. Peera, J. Chattopadhyay, Z. Gu, R. H. Hauge and W. E. Billups, *Nano Lett.*, 2004, **4**, 1257.
34 J. Chattopadhyay, F. De Jesus Cortez, S. Chakaraborty, N. K. H. Slater and W. E. Billups, *Chem. Mater.*, 2006, **18**, 5864.
35 (*a*) G. Viswanathan, N. Chakrapani, H. Yang, B. Wei, H. Chung, K. Cho, C. Y. Ryu and P. M. Ajayan, *J. Am. Chem. Soc.*, 2003, **125**, 9258; (*b*) S. Chen, D. Chen and G. Wu, *Macromol. Rapid Commun.*, 2006, **27**, 882.
36 (*a*) A. Garcia-Gallastegui, I. Obieta, I. Bustero, G. Imbuluzqueta, J. Arbiol, J. I. Miranda and J. M. Aizpurua, *Chem. Mater.*, 2008, **20**, 4433; (*b*) D. Wunderlich, F. Hauke and A. Hirsch, *J. Mater. Chem.*, 2008, **18**, 1493.
37 J. L. Hudson, H. Jian, A. D. Leonard, J. J. Stephenson and J. M. Tour, *Chem. Mater.*, 2006, **18**, 2766.
38 S. Campidelli, B. Ballesteros, A. Filoramo, D. Díaz Díaz, G. de la Torre, T. Torres, G. M. A. Rahman, C. Ehli, D. Kiessling, F. Werner, V. Sgobba, D. M. Guldi, C. Cioffi, M. Prato and J.-P. Bourgoin, *J. Am. Chem. Soc.*, 2008, **130**, 11503.
39 Z. Gho, F. Du, D. Ren, Y. Chen, J. Zheng, Z. Liu and J. Tian, *J. Mater. Chem.*, 2006, **16**, 3021.
40 S. Arepalli, P. Nikolaev, O. Gorelik, V. G. Hadjiev, H. A. Bradlev, W. Holmes, B. Files and L. Yowell, *Carbon*, 2004, **42**, 1783.
41 S. Campidelli, C. Sooambar, E. Lozano-Diz, C. Ehli, D. M. Guldi and M. Prato, *J. Am. Chem. Soc.*, 2006, **128**, 12544.
42 (*a*) M. Burghard, *Surf. Sci. Rep.*, 2005, **58**, 1; (*b*) K. Balasubramanian and M. Burghard, *Small*, 2005, **1**, 180.
43 (*a*) M. S. Dresselhaus, G. Dresselhaus and M. Hofmann, *Vib. Spectrosc.*, 2007, **45**, 71; (*b*) A. Jorio, A. G. Souza Filho, G. Dresselhaus, M. S. Dresselhaus, A. K. Swan, M. S. LnlM, B. B. Goldberg, M. A. Pimenta, J. H. Hafner, C. M. Lieber and R. Saito, *Phys. Rev. B*, 2002, **65**, 155412.
44 (*a*) F. Brunetti, M. Herrero, J. Muñoz, M. Meneghetti, M. Prato and E. Vázquez, *J. Am. Chem. Soc.*, 2008, **130**, 8094; (*b*) F. G. Brunetti, M. A. Herrero, J. d. M. Muñoz, S. Giordani, A. Díaz-Ortiz, S. Filippone, G. Ruaro, M. Meneghetti, M. Prato and E. Vázquez, *J. Am. Chem. Soc.*, 2007, **129**, 14580.
45 X. Liu, T. Pichler, M. Knupfer, M. S. Golden, J. Fink, H. Kataura and Y. Achiba, *Phys. Rev. B*, 2002, **66**, 045411.
46 M. J. O'Connell, S. M. Bachilo, C. B. Huffman, V. C. Moore, M. S. Strano, E. H. Haroz, K. L. Rialon, P. J. Boul, W. H. Noon, C. Kittrell, J. P. Ma, R. H. Hauge, R. B. Weisman and R. E. Smalley, *Science*, 2002, **297**, 593.
47 (*a*) U. J. Kim, C. A. Furtado, X. Liu, G. Chen and P. C. Eklund, *J. Am. Chem. Soc.*, 2005, **127**, 15437 and reference therein; (*b*) J. L. Stevens, A. Y. Huang, H. Peng, I. W. Chiang, V. N. Khabashesku and J. L. Margrave, *Nano Lett.*, 2003, **3**, 331.
48 S. Lebedkin, K. Arnold, F. Hennrich, R. Krupke, B. Renker and M. M. Kappes, *New J. Phys.*, 2003, 5.
49 S. M. Bachilo, M. S. Strano, C. Kittrell, R. H. Hauge, R. E. Smalley and R. B. Weisman, *Science*, 2002, **298**, 2361.
50 L. Cognet, D. A. Tsyboulski, J. D. R. Rocha, C. D. Doyle, J. M. Tour and R. B. Weisman, *Science*, 2007, **316**, 1465.
51 P. H. Tan, A. G. Rozhin, T. Hasan, P. Hu, V. Scardaci, W. I. Milne and A. C. Ferrari, *Phys. Rev. Lett.*, 2007, **99**, 137402.

52 A. Kitaygorodskiy, W. Wang, S.-Y. Xie, Y. Lin, K. A. S. Fernando, X. Wang, L. Qu, B. Chen and Y.-P. Sun, *J. Am. Chem. Soc*., 2005, **127**, 7517.
53 S. J. L. Billinge and I. Levin, *Science*, 2007, **316**, 561.
54 S. Giordani, S. D. Bergin, V. Nicolosi, S. Lebedkin, M. M. Kappes, W. J. Blau and J. N. Coleman, *J. Phys. Chem. B*, 2006, **110**, 15708.
55 Y. W. Fan, M. Burghard and K. Kern, *Adv. Mater*., 2002, **14**, 130.
56 B. R. Azamian, K. S. Coleman, J. J. Davis, N. Hanson and M. L. H. Green, *Chem. Commun*., 2002, 366.
57 L. Zhang, J. Zhang, N. Schmandt, J. Cratty, V. N. Khabashesku, K. F. Kelly and A. R. Barron, *Chem. Commun*., 2005, 5429.
58 T. DeBorde, J. C. Joiner, M. R. Leyden and E. D. Monit, *Nano Lett*., 2008, **8**, 3568.
59 T. W. Odom, J. L. Huang, P. Kim and C. M. Lieber, *Nature*, 1998, **391**, 62.
60 J. W. G. Wildoer, L. C. Venema, A. G. Rinzler, R. E. Smalley and C. Dekker, *Nature*, 1998, **391**, 59.
61 D. Bonifazi, C. Nacci, R. Marega, S. Campidelli, G. Ceballos, S. Modesti, M. Meneghetti and M. Prato, *Nano Lett*., 2006, **6**, 1408.
62 A. Hashimoto, K. Suenaga, A. Gloter, K. Urita and S. Iijima, *Nature*, 2004, **430**, 870.
63 J. M. Zuo, I. Vartanyants, M. Gao, R. Zhang and L. A. Nagahara, *Science*, 2003, **300**, 1419.
64 L. C. Qin, *Rep. Prog. Phys*., 2006, **69**, 2761.
65 R. R. Meyer, S. Friedrichs, A. I. Kirkland, J. Sloan, J. L. Hutchison and M. L. H. Green, *J. Microsc. (Oxford, U. K.)*, 2003, **212**, 152.
66 K. Hirahara, K. Saitoh, J. Yamasaki and N. Tanaka, *Nano Lett*., 2006, **6**, 1778.
67 M. Koshino, T. Tanaka, N. Solin, K. Suenaga, H. Isobe and E. Nakamura, *Science*, 2007, **316**, 853.
68 G. Accorsi, N. Armaroli, A. Parisini, M. Meneghetti, R. Marega, M. Prato and D. Bonifazi, *Adv. Funct. Mater*., 2007, **17**, 2975.

